Transmembrane B-DNA

Naomi Sakai, Bodo Baumeister, and Stefan Matile*[a]

KEYWORDS:

ion channels · membranes · oligonucleotides · protein mimetics · supramolecular chemistry

Transmembrane (TM) intratoroidal space is attracting increasing scientific attention because the spatial compartmentalization by the surrounding bilayer membrane provides vectorial control over and stochastic observability of intratoroidal chemical processes.[1–3] The superb properties of rigid-rod β-barrels[4, 5] have very recently been used to synthesize large transmembrane space of a stability that seemed unique for large biomacromolecules until then.[6] The TM interior of **1**^{6}, characterized by a diameter of 2 – 3 nm and 48 intratoroidal lysine residues, is topologically and electrostatically complementary to Watson – Crick B-DNA (Figure 1). Similar intratoroidal space has been seen within water-soluble DNA-binding proteins such as the 2724-residue hexamer of BH Gal6 comprising 60 intratoroidal lysine residues.[7] The TM intratoroidal space of the paradigmatic 2051-residue heptamer of α hemolysin,[8] on the other hand, has been shown to suffice for the stochastic differentiation of single-stranded homo-DNAs and -RNAs, while double-stranded DNA apparently does not fit.[2] Elucidation of the interaction between B-DNA and the TM intratoroidal space of **1**^{6} seemed thus of potential scientific importance. The combination of the advantageous anisotropy of TM intratoroidal space with the advantageous structural variability of B-DNA may be fruitful with regard to diverse applications, from unidirectional electron transport in "nanodevices"[9–12] to gene transfection[13] and stochastic B-DNA dynamics.[3] Here we report the construction of the first, with all likelihood TM B-DNA as an intratoroidal guest of the formal second-sphere inclusion complex **2**·**3** ⊂ **1**^{6} ⊂ **4**^{n} (Figure 1).

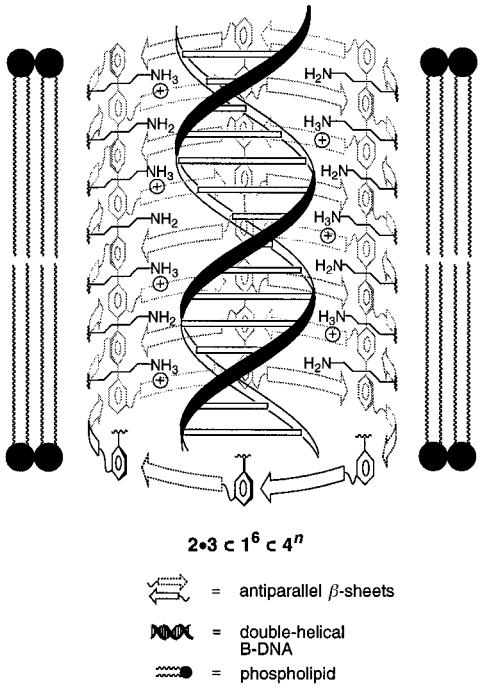

Figure 1. *Schematic structure of second-sphere host – guest complex* **2**·**3** ⊂ **1**^{6} ⊂ **4**^{n} *composed of B-DNA* **2**·**3** *within rigid-rod β-barrel* **1**^{6} *within EYPC bilayers* **4**^{n} *(see Scheme 1 for details). The depicted degree of protonation (ca. 50%) of intratoroidal lysine residues reflects the situation expected in antiparallel β-sheets[28–30] and is consistent with the complementarity of multivalent[31] electrostatic attraction between* **2**·**3** *and* **1**^{6}*, which is possibly further amplified by H-bonding contributions from adjacent amines.[32, 33]*

B-DNA **2**·**3** obtained from d(GT)$_7$ (**2**) and d(CA)$_7$ (**3**) was selected for this study because its length of 43 Å roughly matches the total thickness of EYPC** bilayers **4**^{n}[14] and because of its convenient melting temperature (T_m = 45 °C). The CD spectra of **2**·**3** ⊂ **1**^{6} ⊂ **4**^{n}, prepared by addition of duplexes **2**·**3** to TM nanopores **1**^{6} ⊂ **4**^{n}, were in support of the designed molecular architecture (Scheme 1 A). In fact, the presence of

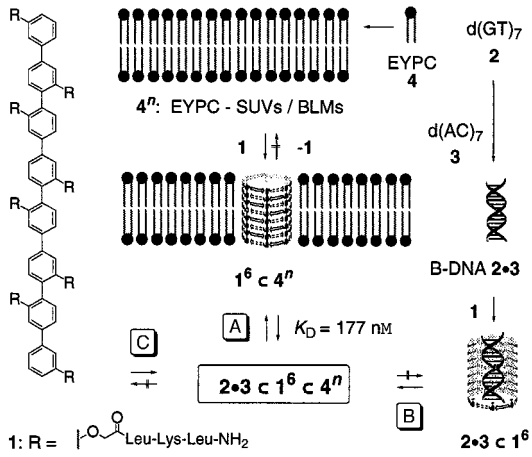

Scheme 1. *Programmed assembly of TM B-DNA* **2**·**3** ⊂ **1**^{6} ⊂ **4**^{n} *by either addition of* **2**·**3** *to* **1**^{6} ⊂ **4**^{n} *(A),* **2**·**3** ⊂ **1**^{6} *to* **4**^{n} *(B), or* **1** *to* **2**·**3** *and* **4**^{n} *(C). Note that the structure of* **2**·**3** ⊂ **1**^{6} *has not been investigated.*

bisignate CD Cotton effects (CEs) centered around the octi-(*p*-phenylene) absorption at 319 nm even at high dilution suggested that barrel **1**^{6} may be further stabilized by > 0.6 mol% of intratoroidal B-DNA templates (Figure 2, solid line).[4–6] CD CEs between 300 and 253 nm, on the other hand, were indicative of intact B-DNA.[16] The binding of topologically mismatched single-stranded oligonucleotides d(GT)$_7$ (**2**) instead of B-DNA **2**·**3** caused destruction of TM nanopores **1**^{6} ⊂ **4**^{n} (Figure 2, dotted line).

Rapid passage of anionic dyes across the interior of TM rigid-rod β-barrel **1**^{6} ⊂ **4**^{n} has been used before to measure the

[a] *Prof. Dr. S. Matile, Dr. N. Sakai, Dipl.-Chem. B. Baumeister*
Department of Organic Chemistry, University of Geneva
Quai Ernest Ansermet 24, 1211 Geneva 4 (Switzerland)
Fax: (+41) 22-328-7396
E-mail: stefan.matile@chiorg.unige.ch

[**] For abbreviations see ref. [15].

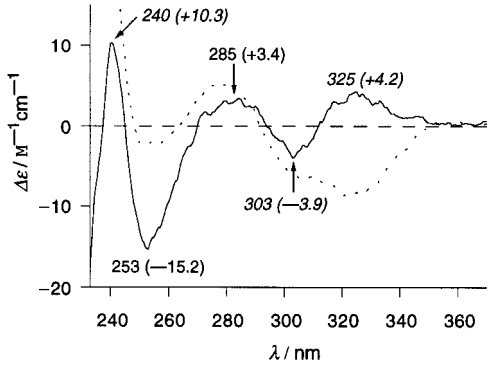

*Figure 2. Representative CD spectra of **1** (6.5 μM) in the presence of EYPC-SUVs **4**^{n} (500 μM **4**) and either B-DNA **2**·**3** (1 μM, solid line) or d(GT)$_7$ **2** (2 μM, dotted line) in 10 mM HEPES, 100 mM NaCl, pH 7.4. CEs indicative of rigid-rod β-barrel **1**^{6} are labeled in italics; dichroic absorptions refer to octi(p-phenylene) concentrations.*

dimensions of its cationic intratoroidal space at nanomolar concentrations.[6, 17] The formation of TM B-DNA **2**·**3** ⊂ **1**^{6} ⊂ **4**^{n} was expected to block dye leakage. Indeed, the addition of one equivalent of B-DNA **2**·**3** fully arrested ongoing CF efflux from EYPC-SUVs through nanopores **1**^{6} ⊂ **4**^{n} that had been assembled immediately before (Scheme 1 A, not shown). To possibly separate the kinetics of TM B-DNA formation from that of dye efflux, different assembly pathways were tested. Addition of mixtures of rods **1** and B-DNA **2**·**3** to EYPC-SUVs **4**^{n} (Scheme 1 B; Figure 3, ●) and addition of **1** to mixtures of **2**·**3** and **4**^{n} (Scheme 1 C; Figure 3, ■) revealed comparable trends: increasing inhibition of dye efflux with increasing duplex concentration (Figure 3, solid lines). The quantitative discrepancies between the two experiments presumably originated from competing, not yet understood interactions between peptide rods **1** and duplexes **2**·**3** in water that complicate the assembly of TM B-DNA **2**·**3** ⊂ **1**^{6} ⊂ **4**^{n} along these routes.

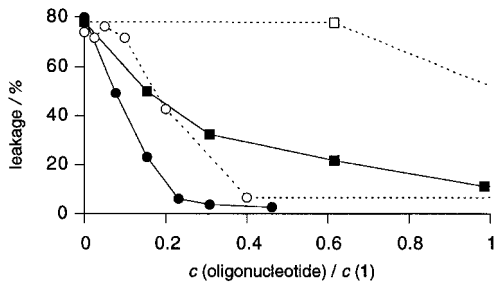

*Figure 3. Blockage of CF efflux through nanopore **1**^{6} ⊂ **4**^{n} by increasing concentrations of B-DNA **2**·**3** (solid lines) and d(GT)$_7$ **2** (dotted lines). ●, ○: Simultaneous addition of **1** and oligonucleotides; ■, □: addition of oligonucleotides before addition of **1**. Conditions were as previously described[6, 17] (EYPC-SUVs (500 μM **4**), **1** (250 nM), 10 mM HEPES, 50 mM CF_{in}, 10 mM $NaCl_{in}$, 107 mM $NaCl_{out}$, pH 7.4, λ_{ex} = 492 nm, λ_{em} = 514 nm).*

Clearly, higher oligonucleotide concentrations were needed to block nanopore **1**^{6} ⊂ **4**^{n} with single-stranded DNA **2** instead of double-stranded DNA **2**·**3** (Figure 3, dotted vs. solid lines). This was consistent with multivalent TM binding of B-DNA **2**·**3** to the complementary intratoroidal space of nanopore **1**^{6} ⊂ **4**^{n}, as suggested by CD spectroscopy (Figure 2). (Although of minor importance for this study, the blockage of **1**^{6} ⊂ **4**^{n} by single-stranded DNA may nevertheless be of scientific interest for the transfer of antisense and antigene drugs.[18–22])

The relative quenching of the emission of oligo(*p*-phenylene) guests by spin-labeled bilayer hosts has been shown to provide precise information on guest location and orientation.[6, 17, 23–25] Figure 4 shows the emission intensities of octi(*p*-phenylene) **1** in labeled and unlabeled EYPC bilayers as a function of time (solid/dotted vs. dashed curves). Notably, the addition of B-DNA **2**·**3** had no effect on rod emission (Figure 4, solid and dashed

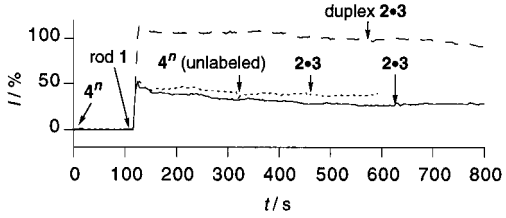

*Figure 4. Representative relative emission intensities of oligo(p-phenylene) **1** (100 nM) in uniformly sized EYPC-SUVs (500 μM **4**) with (solid and dotted lines) and without 8.7% 5-DOXYL-PC (dashed line) as a function of time and the presence of duplex **2**·**3** (16 nM, solid and dashed lines), additional unlabeled EYPC-SUVs (500 μM **4**, dotted line), or both (dotted line) in 10 mM HEPES, 100 mM NaCl, pH 7.4, λ_{ex} = 328 nm, λ_{em} = 390 nm. Conditions were as previously described.[6, 17]*

curves). This corroborated that B-DNA **2**·**3** did not alter the structure of nanopore **1**^{6} ⊂ **4**^{n} (e.g., **2**·**3** ⊂ **1**^{6} ⊂ **4**^{n} ↦ **2**·**3** ⊂ **1**^{6} + **4**^{n}, Scheme 1). No change of rod emission upon the addition of unlabeled SUVs to nanopore **1**^{6} ⊂ **4**^{n} in labeled SUVs (Figure 4, dotted curve) excluded the possibility of intervesicular rod transfer[17] and rod-mediated membrane fusion (e.g., **1**^{6} ⊂ **4**^{n} ↦ **1** + **4**^{n}, Scheme 1). The unchanged situation after subsequent addition of B-DNA **2**·**3** finally proved that the above-mentioned two processes are not induced by TM B-DNA **2**·**3** ⊂ **1**^{6} ⊂ **4**^{n} (Figure 4, dotted curve).

Fluorescence depth quenching experiments thus provided direct evidence that the formation of TM nanopore **1**^{6} ⊂ **4**^{n} and second-sphere complex **2**·**3** ⊂ **1**^{6} ⊂ **4**^{n} is practically irreversible and nondestructive with regard to supramolecular architecture, respectively. The following BLM conductance experiments were in support of these conclusions (Figure 5 A).[26] Multiple, permanently open nanopores **1**^{6} ⊂ **4**^{n} were prepared in EYPC-BLMs as

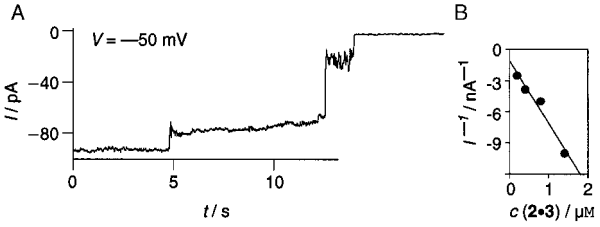

*Figure 5. A: Representative changes in conductance of EYPC-BLMs in the presence of oligo(p-phenylene) **1** as a function of time after the addition of 2.41 μM B-DNA **2**·**3**. B: Steady-state currents I^{-1} as a function of the concentration of B-DNA **2**·**3**. Conditions were as previously described[6] (5 mM HEPES, 2 M NaCl, pH 7.4).*

previously described[6] to give currents I_0 of up to 1 nA in response to an externally applied voltage of -50 mV. Then, different concentrations of B-DNA **2·3** were added to the cis compartment of the BLM to secure unidirectionality between TM B-DNA **2·3** ⊂ **1**^{6} ⊂ **4**^{n} formation and external voltage. Stochastic binding of B-DNA **2·3** to single TM nanopores **1**^{6} ⊂ **4**^{n} was indicated by a stepwise reduction of the initial current I_0 to reach a steady-state current I (Figure 5 A). Nearly complete blockage at high B-DNA concentrations confirmed that these steady-state currents I originated from unoccupied nanopores **1**^{6} ⊂ **4**^{n} at different DNA concentrations and not from the conductivity of TM B-DNA **2·3** ⊂ **1**^{6} ⊂ **4**^{n}. Currents I thus related directly to the fractional occupancy y of **1**^{6} ⊂ **4**^{n} [Eq. (1)], suggesting that the K_D of complex **2·3** ⊂ **1**^{6} ⊂ **4**^{n} [Eq. (2)] could be readily obtained from a plot of I^{-1} as a function of the B-DNA concentration [Eq. (3)].[27]

$$I/I_0 = 1 - y = [\mathbf{1}^6 \subset \mathbf{4}^n]/([\mathbf{2\cdot 3} \subset \mathbf{1}^6 \subset \mathbf{4}^n] + [\mathbf{1}^6 \subset \mathbf{4}^n]) \quad (1)$$

$$K_D = [\mathbf{1}^6 \subset \mathbf{4}^n] \times [\mathbf{2\cdot 3}]/[\mathbf{2\cdot 3} \subset \mathbf{1}^6 \subset \mathbf{4}^n] \quad (2)$$

$$I^{-1} = [\mathbf{2\cdot 3}]/(K_D \times I_0) + I_0^{-1} \quad (3)$$

A dissociation constant $K_D = 177$ nM was obtained (Figure 5 B). Since such a remarkable value[27, 1] impossibly originates from nonspecific ionic interactions at the membrane – water interface, this finding fully confirmed the firm organization and high stability of the supramolecular architecture of TM B-DNA **2·3** ⊂ **1**^{6} ⊂ **4**^{n} (Figure 1).

In summary, the unique properties of rigid-rod β-barrels **1**^{6} have been used to unify biomembranes and B-DNA by refined supramolecular architecture of a remarkable stability exemplified by a K_D value of 177 nM. The obtained B-DNA, which is most likely transmembrane, combines the fundamental advantages of biomembrane anisotropy with the facile structural variability of B-DNA for future use in chemistry, biology, and materials sciences.

We thank the Swiss National Science Foundation (21-57059.99 and NRP 4047-057496) and the Suntory Institute for Bioorganic Research (SUNBOR Grant) for financial support.

[1] L.-Q. Gu, O. Braha, S. Conlan, S. Cheley, H. Bayley, *Nature* **1999**, *398*, 686.
[2] M. Akeson, D. Branton, J. J. Kasianowicz, E. Brandin, D. W. Deamer, *Biophys. J.* **1999**, *77*, 3227.
[3] S. Howorka, L. Movileanu, X. Lu, M. Magnon, S. Cheley, O. Braha, H. Bayley, *J. Am. Chem. Soc.* **2000**, *122*, 2411.
[4] N. Sakai, N. Majumdar, S. Matile, *J. Am. Chem. Soc.* **1999**, *121*, 4294.
[5] B. Baumeister, S. Matile, *Chem. Eur. J.* **2000**, *6*, 1739.
[6] B. Baumeister, N. Sakai, S. Matile, *Angew. Chem.* **2000**, *112*, 2031; *Angew. Chem. Int. Ed.* **2000**, *39*, 1955.
[7] L. Joshua-Tor, H. E. Xu, S. A. Johnston, D. C. Rees, *Science* **1995**, *269*, 945.
[8] L. Song, M. R. Hobaugh, C. Shustak, S. Cheley, H. Bayley, J. E. Gouaux, *Science* **1996**, *274*, 1850.
[9] D. Porath, A. Bezryadin, S. de Vries, C. Dekker, *Nature* **2000**, *403*, 635.
[10] M. Nunez, D. B. Hall, J. K. Barton, *Nature* **1996**, *382*, 731.
[11] E. Meggers, M. E. Michel-Beyerle, B. Giese, *J. Am. Chem. Soc.* **1998**, *120*, 12950.
[12] P. T. Henderson, D. Jones, G. Hampikian, G. Kan, B. G. Schuster, *Proc. Natl. Acad. Sci. USA* **1999**, *96*, 8353.
[13] J.-P. Behr, *Acc. Chem. Res.* **1993**, *26*, 274.
[14] A. M. Kleinfeld, *Curr. Top. Membr. Transp.* **1987**, *29*, 1.
[15] Abbreviations and reagents: BLM = black lipid membrane, CF = 5(6)-carboxyfluorescein (Fluka), DOXYL = 4,4-dimethyl-3-oxazolinyloxyl, 5-DOXYL-PC = 1-palmitoyl-2-stearoyl(5-DOXYL)-*sn*-glycero-3-phosphocholine (Avanti Polar Lipids), EYPC = egg yolk phosphatidylcholine (Northern Lipids Inc.), HEPES = 2-[4-(2-hydroxyethyl)-1-piperazinyl]ethanesulfonic acid, SUV = small unilamellar vesicle.
[16] W. C. Johnson in *Circular Dichroism—Principles and Applications* (Eds.: K. Nakanishi, N. Berova, R. W. Woody), VCH, Weinheim, **1994**, pp. 523 – 540.
[17] L. A. Weiss, N. Sakai, B. Ghebremariam, C. Ni, S. Matile, *J. Am. Chem. Soc.* **1997**, *119*, 12142.
[18] T. B. Wyman, F. Nicol, O. Zelphati, P. V. Scaria, C. Plank, F. C. Szoka, Jr., *Biochemistry* **1997**, *36*, 3008.
[19] J. Dufourcq, W. Neri, N. Henry-Toulmé, *FEBS Lett.* **1998**, *421*, 1.
[20] T. Niidome, N. Ohmori, A. Ichinose, A. Wada, H. Mihara, T. Hirayama, H. Aoyagi, *J. Biol. Chem.* **1997**, *272*, 15307.
[21] P. S. Miller in *Bioorganic Chemistry—Nucleic Acids* (Ed.: S. M. Hecht), Oxford University Press, Oxford, **1996**, pp. 347 – 374.
[22] P. E. Nielsen, G. Haaima, *Chem. Soc. Rev.* **1997**, 73.
[23] N. Sakai, S. Matile, *Chem. Eur. J.* **2000**, *6*, 1731.
[24] J. Ren, S. Lew, Z. Wang, E. London, *Biochemistry* **1997**, *36*, 10213.
[25] A. S. Ladokhin, *Methods Enzymol.* **1997**, *278*, 462.
[26] B. Hille, *Ionic Channels of Excitable Membrane*, 2nd ed., Sinauer, Sunderland, MA, **1992**.
[27] see ref. [26], pp. 59 – 82.
[28] J. P. Schneider, J. W. Kelly, *Chem. Rev.* **1995**, *95*, 2169.
[29] J. S. Nowick, *Acc. Chem. Res.* **1999**, *32*, 287.
[30] C. K. Smith, L. Regan, *Acc. Chem. Res.* **1997**, *30*, 153.
[31] M. Mammen, S.-K. Choi, G. M. Whitesides, *Angew. Chem.* **1998**, *110*, 2908; *Angew. Chem. Int. Ed.* **1998**, *37*, 2754.
[32] A. D. Hamilton, V. Jubilan, R. P. Dixon, *J. Am. Chem. Soc.* **1992**, *114*, 1120.
[33] E. V. Anslyn, J. Smith, K. Ariga, *J. Am. Chem. Soc.* **1993**, *115*, 362.

Received: April 18, 2000 [Z 44]